

Nuclear export protein CSE1L interacts with P65 and promotes NSCLC growth via NF- κ B/MAPK pathway

H.C. Lin,^{1,4} J. Li,^{2,4} D.D. Cheng,³ X. Zhang,¹ T. Yu,¹ F.Y. Zhao,¹ Q. Geng,¹ M.X. Zhu,¹ H.W. Kong,¹ H. Li,¹ and M. Yao¹

¹State Key Laboratory of Oncogenes and Related Genes, Shanghai Cancer Institute, Renji Hospital, Shanghai Jiao Tong University School of Medicine, Shanghai 200032, China; ²Department of Oncology, Huashan Hospital, Fudan University, Shanghai 200040, China; ³Department of Orthopedics, Shanghai Jiao Tong University Affiliated Sixth People's Hospital, Shanghai 200233, China

Non-small cell lung cancer (NSCLC) is characterized with high morbidity and mortality, mainly due to frequent recurrence and metastasis. However, the underlying molecular mechanisms of NSCLC tumorigenesis are largely unclear. Through data mining in the ONCOMINE and Gene Expression Omnibus (GEO) databases, the expression of CSE1L (chromosome segregation like 1 protein/CAS), an exportin, was identified to be significantly upregulated in NSCLC and positively associated with poor prognosis of patients. By use of *in vitro* and *in vivo* gain-and loss-of-function experiments, we found that CSE1L can promote NSCLC cell proliferation while inhibiting cell apoptosis. Through immunoprecipitation and mass spectrometry experiments, we demonstrated that CSE1L interacted with RELA (named as P65) and affected its location in the nucleus. Moreover, we found that one of the mechanisms by which CSE1L promotes proliferation and inhibits apoptosis is through activating the nuclear factor- κ B (NF- κ B)/mitogen-activated protein kinase (MAPK) signaling pathway. In summary, our findings indicated an oncogenic role of CSE1L in NSCLC tumorigenesis.

INTRODUCTION

According to global cancer statistics, lung cancer is the most commonly diagnosed cancer and the leading cause of cancer death.¹ Non-small cell lung cancer (NSCLC), including squamous cell carcinoma, adenocarcinoma, and large cell carcinoma, accounts for approximately 85% of lung cancer cases.^{2,3} Recently, molecular-targeted therapies, such as epidermal growth factor receptor (EGFR) gene mutations and anaplastic lymphoma kinase (ALK) gene rearrangement,^{4,5} have opened a new era in the management of lung cancer.⁶ However, due to the lack of therapeutic means, non-resectable and recurrent lung adenocarcinoma mostly have an unfavorable prognosis and a low survival rate.⁷ Hence, it has been an urgent need to identify potential therapeutic targets in order to improve the outcome of NSCLC.

Small molecules tend to passively diffuse through the nuclear pore complex (NPC), whereas larger cargoes, such as mRNA and specific

proteins, require various transport receptors.^{8,9} Nuclear transport receptors (NTRs) are also called karyopherins, including importins, exportins, and transportin(s). There are more than 20 kinds of NTRs in eukaryotes.^{10,11} Export and import of mRNA and specific proteins from the nucleus is a key step in intracellular signaling and affects cell proliferation or apoptosis. Cancer cells facilitate nuclear-cytoplasmic transport through the NPC to stimulate tumor growth and effectively evade apoptosis.¹² NTRs inhibitors have shown preclinical anticancer activity and been considered as potential therapeutic targets in cancer treatment.¹³ The development of specific inhibitors for importins is challenging, and many efforts have been made for their transition into clinical trials.¹⁴ In contrast, the development of exportin inhibitors has evolved at a quicker pace. XPO1 (exportin-1/chromosome region maintenance 1/CRM1) is the main mediator of nuclear export in many cell types,¹⁵ and its inhibitor Selinexor was approved by the FDA approval in the treatment of multiple myeloma (MM) and diffuse large B cell lymphoma (DLBCL).¹⁶ Targeting the key mediators of nucleocytoplasmic transport in cancer cells represents a novel strategy in cancer intervention and possesses the potential for clinical trials.

Here, the ONCOMINE database (<https://www.oncomine.org/resource/login.html>) and Gene Expression Omnibus (GEO) database (<https://www.ncbi.nlm.nih.gov/geo/query/acc.cgi>) were utilized to screen NSCLC-related NTRs, and CSE1L (chromosome segregation like 1 protein) was found out to be the best candidate. We found that CSE1L expression was upregulated in human NSCLC tissues

Received 27 January 2021; accepted 6 March 2021;
<https://doi.org/10.1016/j.omto.2021.02.015>.

⁴These authors contributed equally

Correspondence: Ming Yao, State Key Laboratory of Oncogenes and Related Genes, Shanghai Cancer Institute, Renji Hospital, Shanghai Jiao Tong University School of Medicine, Shanghai 200032, China.

E-mail: myao@shsci.org

Correspondence: Hong Li, State Key Laboratory of Oncogenes and Related Genes, Shanghai Cancer Institute, Renji Hospital, Shanghai Jiao Tong University School of Medicine, Shanghai 200032, China.

E-mail: hongli@shsci.org



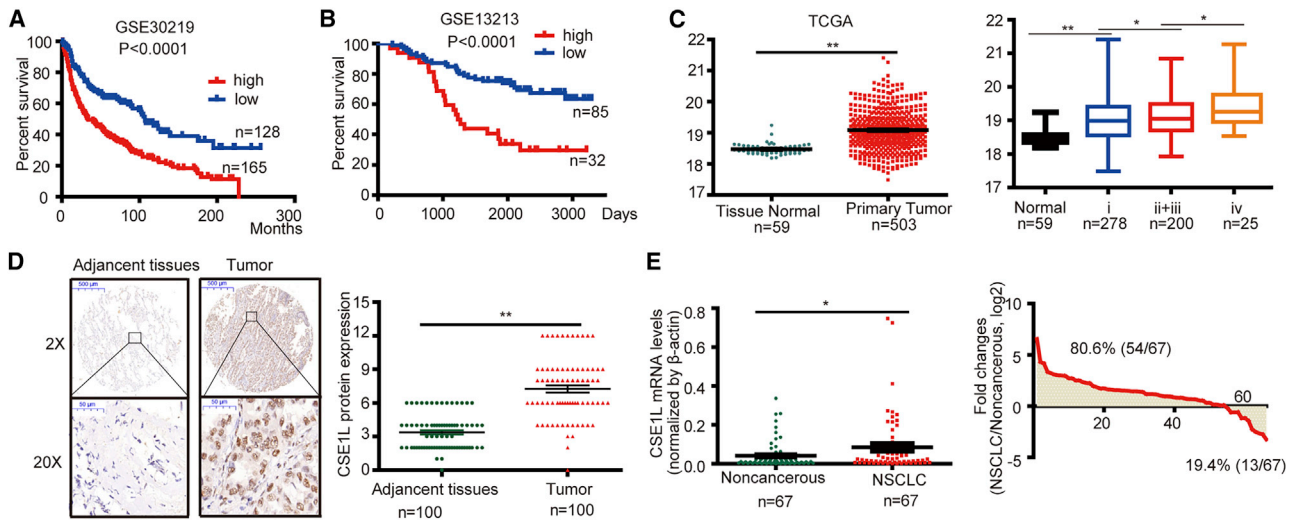


Figure 1. CSE1L is upregulated in NSCLC and correlated with the poor outcome

(A) The survivals of CSE1L in GEO: GSE30219. (B) The survivals of CSE1L in GEO: GSE13213. (C) The expression of CSE1L in 59 normal tissues and 503 lung adenocarcinoma patients TCGA cohort (left), and the correlation between CSE1L mRNA levels and NSCLC patients' TNM stages (right). (D) The representative of IHC staining images for CSE1L of tumor and adjacent tissues are shown in the left and the statistics scores is in the right. (E) The CSE1L mRNA levels were quantified in 67 pairs of NSCLC tissues and noncancerous by using real-time PCR (left), and the fold changes of CSE1L expression in 67 paired tissues (right). Error bars represent the SEM and the min to mix. * $p < 0.05$; ** $p < 0.01$.

and its high expression correlated with a worse outcome. Next, we manipulated CSE1L expression and assessed the effects on cell proliferation, apoptosis, and tumor growth *in vitro* and *in vivo*. Mechanically, coimmunoprecipitation (coIP) and proteomic analyses we identified implied that CSE1L interacted with P65 and affected its expression and nuclear stabilization. Lastly, the mitogen-activated protein kinase (MAPK) signal pathway responsible for P65 regulation in response to CSE1L-induced tumor progression was also explored. In summary, the nuclear exportin CSE1L may serve as a potential therapeutic target in NSCLC.

RESULTS

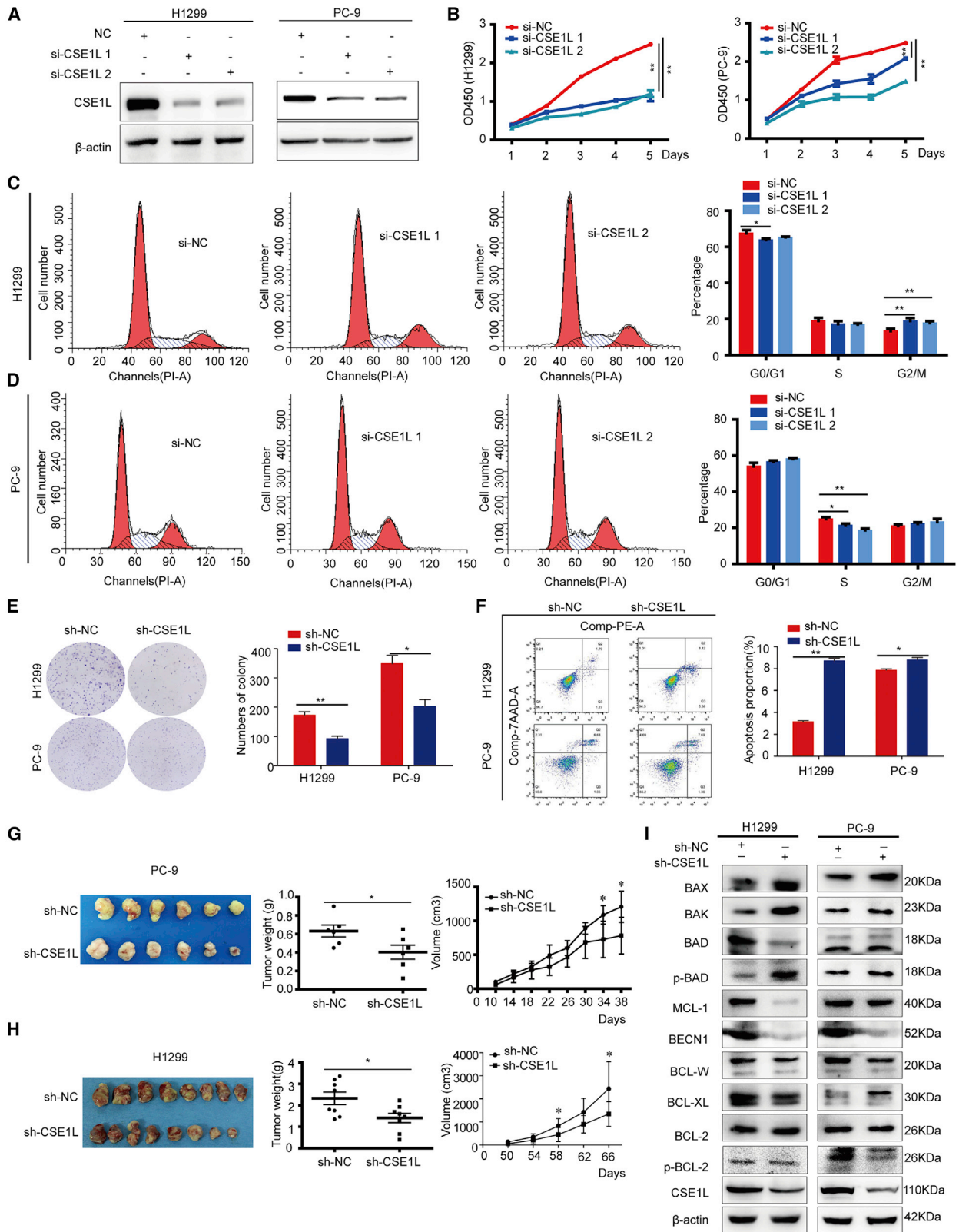
CSE1L upregulated in NSCLC and associated with poor outcomes

We screened NSCLC-related NTRs by utilizing the ONCOMINE database and GEO database. First, we analyzed the mRNA expression of 24 NTRs in lung cancers from the ONCOMINE database. 7 NTRs (KPNA2, TNPO1, IPO13, XPO1, CSE1L, XPO5, XPOT) exerted higher mRNA expression in patients with lung cancer, while 17 NTRs (KPNA1, KPNA3, KPNA4, KPNA5, KPNA6, KPNB1, TNPO2, TNPO3, IPO4, IPO5, IPO7, IPO8, IPO9, IPO11, XPO4, XPO6, XPO7) showed no significant difference in expression compared with normal lung tissues (Figure S1A). Next, we analyzed the clinical relevance of the 7 nuclear transporters in the GEO database (GEO: GSE30219 and GSE13213) and found that higher expression levels of CSE1L and XPO5 were significantly associated with a worse outcome of lung cancer patients (Figures S1B and S1C; Figures 1A and 1B). However, there is no significant difference between the patient outcome and expression levels of expression level of KPNA2, TNPO1, XPO1, and XPOT in GEO: GSE30219 cohort and

IPO13 in GEO: GSE13213 cohort. Taken together, the results revealed that higher expression of CSE1L and XPO5 might associate with the lung cancer. XPO5 has been reported to promote lung cancer cell proliferation and apoptosis previously,^{17,18} while the role of CSE1L in NSCLC remains unknown. Therefore, CSE1L was selected for further investigation in the current study.

To further assess the clinical significance of CSE1L, we examined the correlation between CSE1L mRNA expression levels and NSCLC clinicopathological features in an independent The Cancer Genome Atlas (TCGA) cohort with 503 lung adenocarcinoma patients. The expression of CSE1L was observed to be highly increased in tumor tissues compared with adjacent non-tumor lung tissues. Importantly, increased CSE1L expression was positively correlated with advanced pathological tumor node metastasis

(TNM) stages (Figure 1C). Next, we examined CSE1L protein by immunohistochemistry (IHC) assay in a NSCLC tissue microarray, which contained 100 pairs of NSCLC tissues and matched normal tissues. The representative IHC staining results are shown in Figure 1D. The IHC results showed that CSE1L was significantly overexpressed in tumor tissues compared to the matched normal tissues. However, the clinical analysis showed that the protein expression level of CSE1L had no correlation with gender, age, histological grade, clinical stage, and T/N stage (Table S1). Next, we analyzed CSE1L mRNA expression level in another 67-pair human NSCLC and their corresponding noncancerous lung tissues by real-time polymerase chain reaction (PCR). Compared with corresponding noncancerous tissues, CSE1L was significantly upregulated in NSCLC tissues. Moreover, the mRNA expression level of CSE1L was upregulated in 80.6% (54/67)



(legend on next page)

of NSCLC cases (Figure 1E). The mRNA expression level of CSE1L had no correlation with other clinicopathologic characteristics (Table S2). To investigate the functional roles of CSE1L in NSCLC cells, we detected the mRNA and protein levels of CSE1L in NSCLC cell lines (Figures S2A and S2B). Taken together, our data showed that CSE1L was highly expressed in NSCLC and associated with poor outcomes.

CSE1L exerted a promoting effect on NSCLC *in vitro* and *in vivo*

First, we attenuated the expression of CSE1L using small interfering RNAs (siRNAs; Figure 2A) and established stable cellular models of CSE1L overexpression in A549 and H292 cell lines (Figure 3A). Cell Counting Kit-8 (CCK-8) assays indicated that CSE1L knockdown significantly inhibited the proliferation of NSCLC cells (Figure 2B), whereas overexpression of CSE1L substantially promoted the proliferative abilities (Figure 3B). Cell-cycle analysis demonstrated that the percentage of cells in G2/M phase increases in H1299 cells and the percentage of cells in S phase reduces in PC-9 cells after CSE1L knockdown (Figures 2C and 2D), whereas the percentage of cells in G0/G1 and S phase increases and G2/M reduces in A549 cells upon CSE1L overexpression (Figure 3C). Moreover, knockdown of CSE1L significantly inhibited the cell migratory and invasive potential in PC-9 and H1299 cells ($p < 0.05$, Figures S3A and S3B). Moreover, we established stable cellular models of CSE1L knockdown in H1299 and PC-9 cell lines (Figures S2C and S2D) and found that knockdown of CSE1L inhibits cell growth, whereas CSE1L overexpression shows the opposite result (Figures 2E and 3D). Moreover, CSE1L knockdown promoted apoptosis, whereas CSE1L overexpression suppressed apoptosis in NSCLC cells (Figures 2F and 3E). To evaluate the effect of CSE1L *in vivo*, we used mouse xenograft models. The results showed a lower tumor growth rate in small hairpin (sh)-CSE1L groups than negative control group, with smaller tumor volumes and lower tumor weights ($p < 0.05$; Figures 2G and 2H). In contrast, stable overexpression of CSE1L significantly increased the tumor volumes and tumor weights compared to the control groups ($p < 0.05$; Figures 3F and 3G). There was no significant difference between the four groups in terms of body weight (Figure S4). Furthermore, we found that CSE1L knockdown suppresses the expression of apoptosis-related proteins, including p-BCL-2, BCL-XL, BCL-W, BECN1, and MCL-1, while inducing the expression of BAX, BAK, and p-BAD (Figure 2E). In conclusion, these results indicated that CSE1L promoted NSCLC development both *in vitro* and *in vivo*.

CSE1L interacted with P65 and stabilizes P65 in the nucleus

A vast number of studies have suggested that CSE1L acted as oncogene in tumor development, but the role of CSE1L in NSCLC has

not been explored clearly. In this study, coIP combined with mass spectrometry (MS) analysis were used to screen the potential interacted protein with CSE1L. coIP samples of CSE1L extracted from H1299 and PC-9 cells were examined in SDS-PAGE followed by silver staining, and the location of CSE1L was indicated (Figure S5A). Next, the coIP samples were subjected to in-gel trypsin digestion and extracted to MS analysis. MS analysis identified eight proteins (UBC, P65, RAN, KPNB1, mutS homolog 6 [MSH6], SSBP1, CTPS2, and ATP50) that might interact with CSE1L in H1299 and PC-9 cells (Figure S5B). As CSE1L was identified as a nucleoprotein in the Uniprot, we gave priority to the proteins located in nucleus. Interestingly, the protein MSH6 was previously verified to bind with CSE1L,¹⁹ so we turned to the other four nuclear proteins for further study. We found that P65 could interact with CSE1L in H1299, PC-9, and 293T cells but not RAN, UBC, and KPNB1 (Figure S5C; Figure 4A). Meanwhile, CSE1L was determined from IP isolated by P65 antibody in H1299, PC-9, and 293T cells (Figure 4A). Immunofluorescence assay showed co-localization of CSE1L and P65 in NSCLC cells (Figure 4B). This evidence collectively indicated an endogenous interaction between CSE1L and P65. To further study the mechanism of this interaction between CSE1L and P65, we attenuated the expression of CSE1L and P65, respectively. Western blot (WB) showed a significant decrease in P65 protein expression with CSE1L attenuation. In contrast, P65 was increased when CSE1L expression went up (Figure 4C). However, there were few significant changes in the mRNA level of P65 after CSE1L knockdown or overexpression (Figure S5D). Then we performed a nuclear and cytoplasmic separation test, we found that the nuclear proportion of P65 was reduced in CSE1L knockdown cells while CSE1L remained unchanged with P65 knockdown (Figures 4D and 4E). The immunofluorescence assay also reached similar results (Figure 4F). These data indicated that P65, as a downstream protein, was regulated by CSE1L in the nucleus rather than the cytoplasm. After cycloheximide (CHX) blocked protein synthesis, the half-life of P65 protein in CSE1L knockdown cells was significantly shorter than the control cells; in contrast, the half-life of P65 protein in CSE1L-overexpressed cells was longer than the control cells (Figures 4G and 4H). Taken together, this evidence demonstrated that CSE1L interacted with P65 in the nucleus and facilitated the stabilization of P65.

CSE1L promoted cell proliferation and inhibited apoptosis partly through P65

Our findings demonstrated that CSE1L could promote cell proliferation and inhibit cell apoptosis. However, the way that CSE1L affected NSCLC development remained largely unknown. We first introduced

Figure 2. Effects of knockdown of CSE1L on NSCLC cell proliferation and apoptosis

(A) The protein expression levels of CSE1L in CSE1L knockdown and negative control H1299 and PC-9 cells were determined by western blotting analysis. (B) The effect of si-CSE1L on cell proliferation was evaluated by a CCK-8 assay in H1299 and PC-9 cells. (C and D) Flow cytometry was employed to detect the cell cycle after si-CSE1Ls in (C) H1299 cells and (D) PC-9 cells. (E) The effect of knockdown CSE1L on cell proliferation was evaluated by a colony-formation assay in H1299 and PC-9 cells. (F) Flow cytometry was employed to detect the apoptosis percentages of the CSE1L knockdown cells and control cells. (G and H) The xenograft tumors formed by the sh-CSE1L targeted and negative control H1299 and PC-9 cells. The weight of the xenograft tumors and the growth curve demonstrating the tumor volumes on indicated days were shown in the middle and the right. (I) WB was used to detect the apoptotic-related markers in CSE1L knockdown H1299 and PC-9 cells. Error bars represent the SEM and SD. * $p < 0.05$; ** $p < 0.01$.

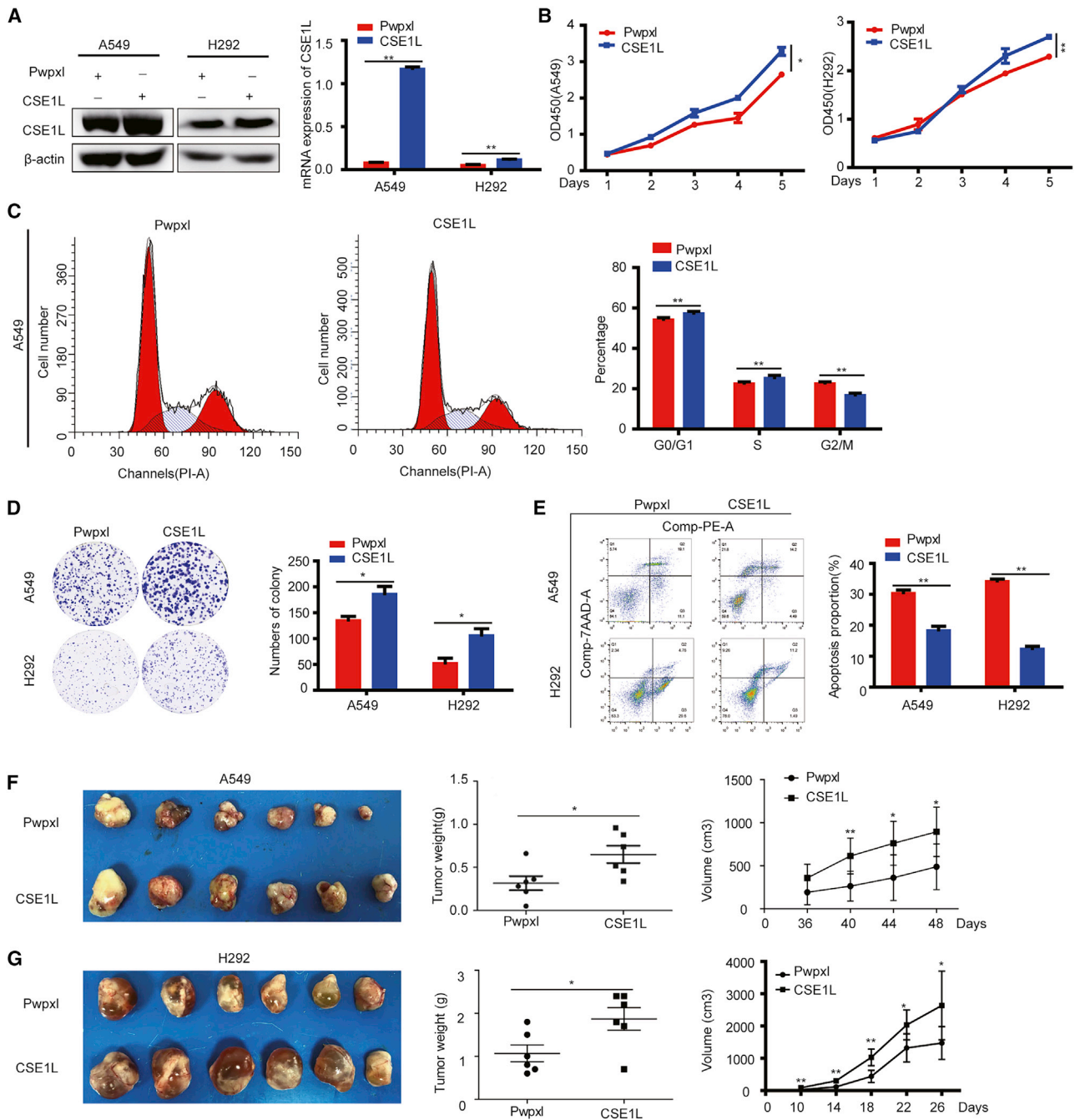


Figure 3. Effects of overexpression of CSE1L on NSCLC cell proliferation and apoptosis

(A) The mRNA and protein levels of CSE1L in CSE1L overexpression and negative control A549 and H292 cells were determined by real-time PCR and western blotting analyses, respectively. (B) The effect of CSE1L on cell proliferation was evaluated by a CCK-8 assay in A549 and H292 cells. (C) Flow cytometry was employed to detect the cell cycle of the CSE1L-overexpression cells and control cells. (D) The effect of CSE1L on cell proliferation was evaluated by a colony-formation assay in A549 and H292 cells. (E) Flow cytometry was employed to detect the apoptosis percentages of the CSE1L-overexpression cells and control cells. (F and G) The xenograft tumors formed by the sh-CSE1L targeted and negative control A549 and H292 cells. The weight of the xenograft tumors and the growth curve demonstrating the tumor volumes on indicated days were shown in the middle and the right. Error bars represent the SEM and SD. * $p < 0.05$; ** $p < 0.01$.

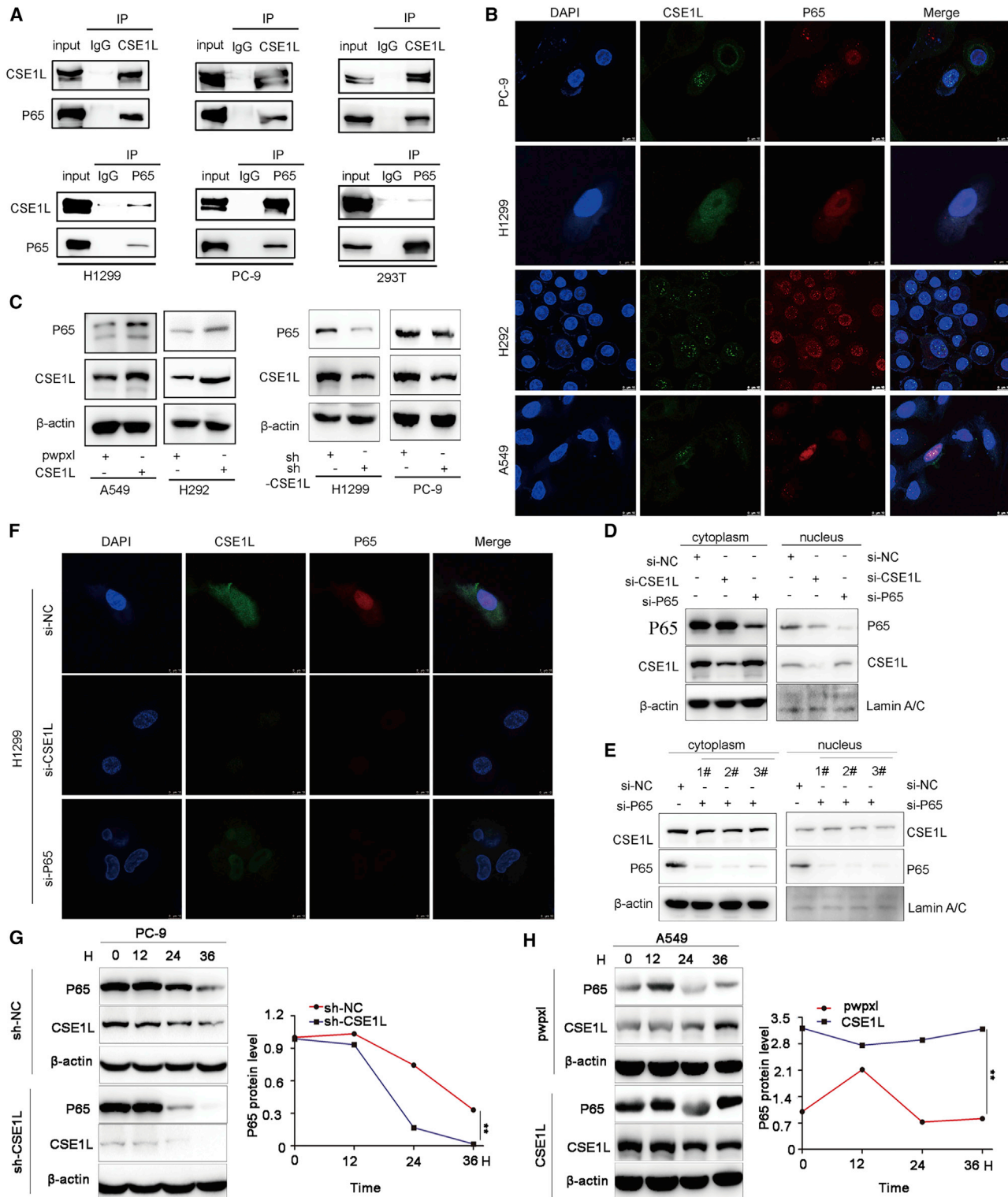


Figure 4. CSE1L interacted with P65 and stabilized the P65 protein expression in NSCLC cells
 (A) colIP was carried out using an anti-CSE1L antibody (upper diagram) or anti-P65 antibody (lower diagram). The immunoblotting assay detected anti-CSE1L and anti-P65 antibodies, respectively. IgG was used as a negative control. (B) Immunofluorescence staining was used to detect the colocalization and co-expression of the CSE1L and

(legend continued on next page)

P65-specific siRNA to knock down in H1299 and PC-9 cells (Figure 5A) and carried out the CCK-8 and apoptosis assays. The results demonstrated that P65 knockdown exhibited a similar effect as CSE1L attenuation in NSCLC cells (Figures 5B and 5C). Since CSE1L interacted with P65 and affected its protein expression and stability in NSCLC cells, it was plausible that CSE1L might function through regulating P65. To confirm this hypothesis, we silenced P65 in CSE1L-overexpressed A549 and H292 cells (Figures 5D and 5E). Then, colony formation and apoptosis assays were applied to observe influences. We found that P65 knockdown significantly inhibited the enhanced growth induced by CSE1L overexpression (Figures 5F and 5G) and aggravated cell apoptosis of relieved by CSE1L overexpression (Figures 5H and 5I). In summary, this evidence revealed that CSE1L promoted cell proliferation and inhibited apoptosis through P65.

CSE1L regulated P65 and promoted NSCLC progression by activating the nuclear factor- κ B (NF- κ B)/MAPK signaling pathway

Investigations are still needed for the CSE1L-associated signaling pathways that are responsible for mediating human lung cancer cell proliferation and apoptosis. To further elucidate this, we utilized RNA sequencing (RNA-seq) to elucidate the altered transcriptional profiles after CSE1L knockdown. The Kyoto Encyclopedia of Genes and Genomes (KEGG) pathway analysis for RNA-seq results indicated that multiple pathways got involved, such as MAPK signaling pathway, p53 signaling pathway, apoptosis, ferroptosis, and tumor necrosis factor (TNF) signaling pathway (Figure 6A). Meanwhile, gene set enrichment analysis (GSEA) was utilized to reveal the gene signature affected by CSE1L downregulation. The process of apoptosis and TNF signaling pathway were enriched by GSEA (Figures 6B and 6C). The results of qRT-PCR experiments confirmed that the apoptosis process and TNF signaling pathway were significantly affected after CSE1L interference (Figures 6D and 6E). Moreover, it was proved that CSE1L interacted with P65, which was a key protein in the MAPK signaling pathway and TNF signaling pathway (Figure 6F). To further verify these results, we used WB to detect the expression of related proteins in the MAPK signaling pathway in NCI-H1299 cells with CSE1L knockdown and in A549 cells with CSE1L overexpression. The results showed that the apoptosis-associated molecules such as p-JNK, ITCH, CREB, caspase-8, caspase-3, and caspase-7 were obviously changed, and the MKK7 and total of JNK protein levels were not significantly altered (Figure 6G). Meanwhile, the protein levels of p-MEK1/2, p-ERK1/2, and p-MSK1 were significantly altered, while the total of MEK1/2, ERK1/2, and MSK1 proteins remained unchanged (Figure 6H). The results indicated that CSE1L could regulate the protein expression level of P65 and promote cell proliferation and inhibit apoptosis through the NF- κ B/MAPK signaling pathway.

High expression of CSE1L and P65 significantly associated with worse prognosis of NSCLC patients

To determine whether the expression of CSE1L and P65 in NSCLC were related to the prognosis of patients with lung cancer, we performed WB analysis in 40-pair cancer and corresponding noncancerous tissues from NSCLC patients. The expression levels of CSE1L and P65 in the 40 NSCLC tissues were higher than those in adjacent noncancerous tissues (Figure 7A). Within 40 NSCLC specimens, high expression of CSE1L was found in 33 cases of NSCLC (82.5%), and high expression of P65 was found in 35 cases of NSCLC (87.5%; Figure 7B). Noticeably, protein expression of CSE1L was positively correlated with P65, suggesting a potential CSE1L-P65 axis in lung cancer tissues ($R = 0.7794$, $p < 0.0001$; Figure 7C). The analysis of protein expression level of CSE1L and P65 in 7 NSCLC cell lines also reached similar results ($R = 0.9262$, $p = 0.0027$; Figure 7D). Moreover, CSE1L protein expression was positively correlated with P65 in a tissue microarray with 25 lung adenocarcinomas ($R = 0.4699$, $p = 0.0178$; Figure 7E). The protein expression level of P65 was significantly correlated with histological grade (Table S3). To further explore the role of P65 in prognostic prediction, we analyzed the P65 expression from the publicly available GEO database (GEO: GSE13213, $n = 117$). The survival analysis showed that higher expression levels of P65 indicated shorter survival times for lung cancer patients (Figure 7F). The receiver operating characteristic (ROC) curves illustrated that the areas under the curve of the CSE1L- and P65-based predictions were 0.660 and 0.612, respectively, suggesting that they could both potentially be applied for the prediction of patient outcome (Figure S6). To further explore the predictive role of CSE1L and P65 in cancer prognosis, we analyzed the mRNA expression level of CSE1L and P65 and the corresponding clinical data from the publicly available GEO database (GEO: GSE13212, $n = 117$). Interestingly, the shortest survival time was observed in the group with the higher expression of both CSE1L and P65 (Figure 7G), and the ROC curve of CSE1L and P65 was 0.674 (Figure S5D). Taken together, these findings indicate that CSE1L-P65 might serve as potential prognostic biomarkers for lung cancer.

DISCUSSION

As a key factor in the nuclear transport pathway, CSE1L is the human homolog of the yeast gene CSE1 that contains a 971-amino acid (aa) open reading frame, and encodes a protein that distributes in the cell nuclei and cytoplasm.²⁰ The DNA fragment was first isolated by Brinkmann et al.²¹ in 1995 in MCF-7 breast cancer cells. CSE1L was found to play roles in apoptosis, cell proliferation and survival,²² microvesicle formation,²³ nucleocytoplasmic transport,²⁴ and cancer metastasis.^{25,26} The CSE1L gene maps to 20q13, a locus that is often amplified in various kinds of cancer and is associated with genetic instability.²⁷ CSE1L is highly expressed in tissues with a high mitotic index such as human tumor cells,²⁸ fetus liver, and testes, and CSE1L expression is correlated

P65 proteins in the nucleus. (C) The regulatory relationship between CSE1L and P65 was verified by western blotting. (D and E) Nuclear and cytoplasmic separation test was carried out to measure the expression of CSE1L and p65 in the nucleus and cytoplasm of si-CSE1L or si-P65. β -actin and lamin A/C were used as an internal control. (F) Immunofluorescence staining was used to detect the colocalization of si-CSE1L or si-P65. (G) PC-9 cells with CSE1L knockdown and (H) A549 cells overexpressing CSE1L were treated with CHX (100 μ g/mL) for the indicated time points. The cell lysates were examined by western blot. Error bars represent the SEM and SD. * $p < 0.05$; ** $p < 0.01$.

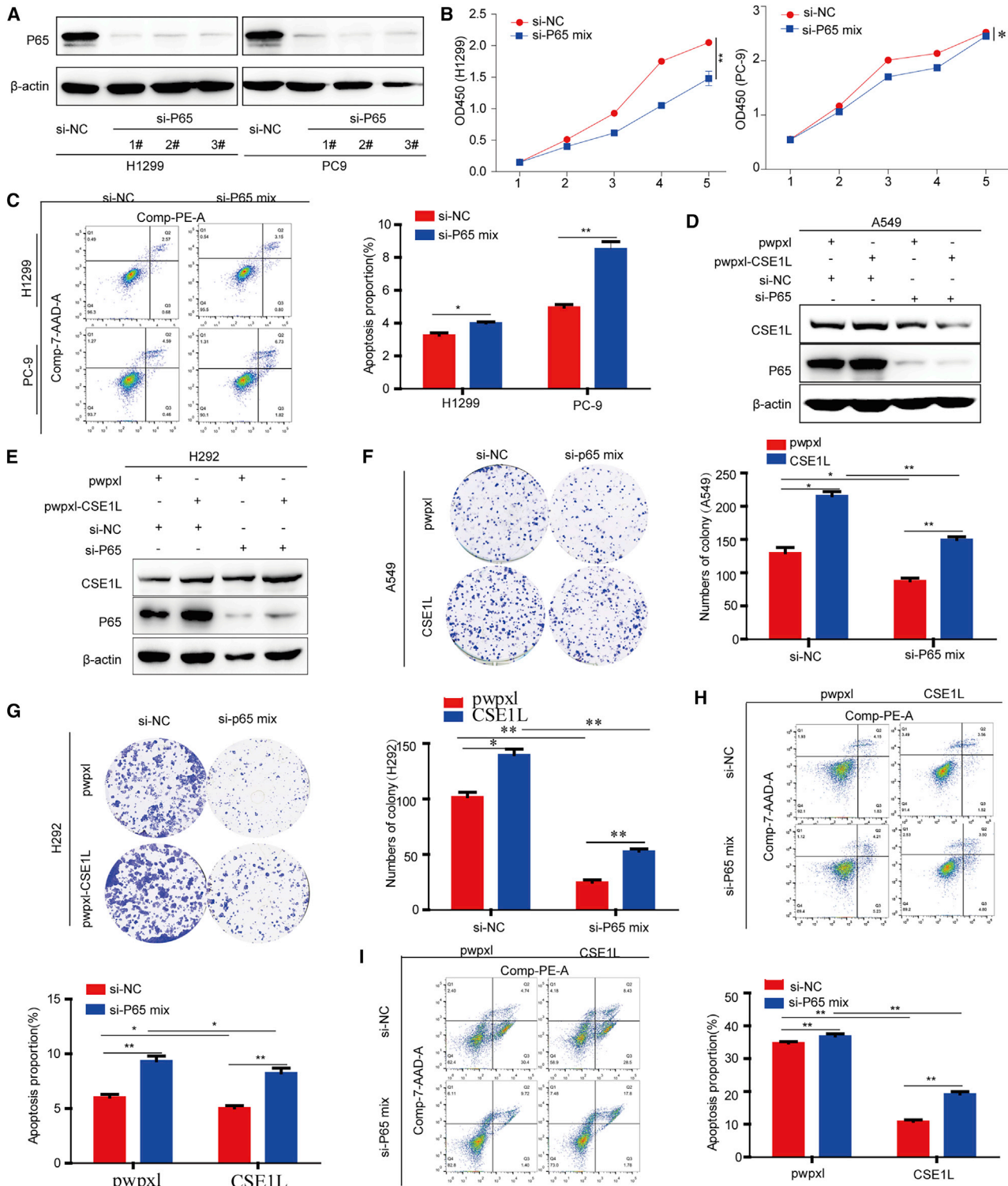


Figure 5. CSE1L promoted cell proliferation and inhibited apoptosis possibly via P65

(A) Confirmation of protein expression levels following si-P65 transfection by western blotting in H1299 and PC-9 cells (B) CCK-8 assay was performed to detect tumor cell proliferation after si-P65 mix transfection in H1299 and PC-9 cells. (C) Flow cytometry was employed to detect the apoptosis percentages after si-P65 mix transfection in

(legend continued on next page)

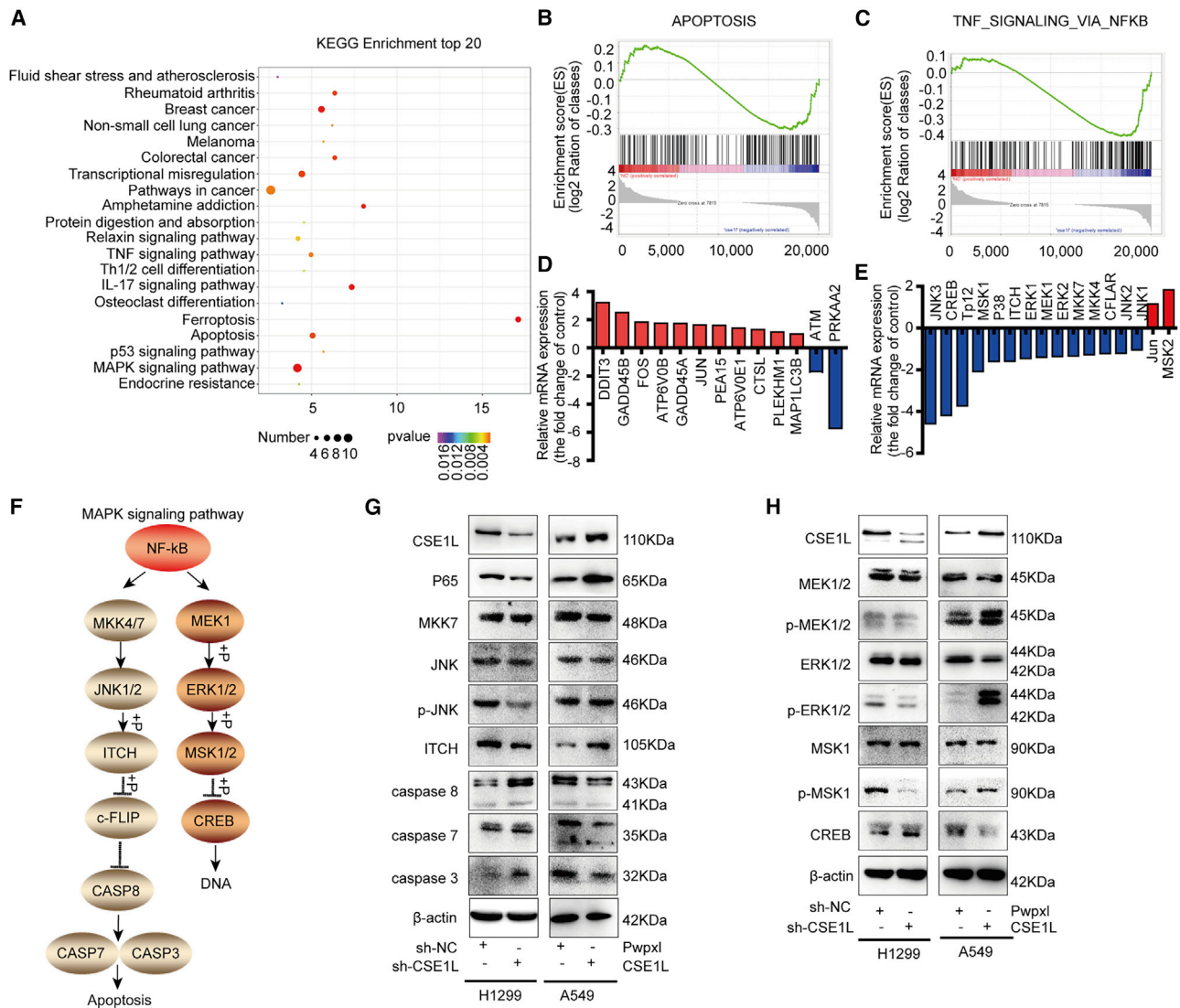


Figure 6. CSE1L regulated P65 and promoted NSCLC cell proliferation and inhibited apoptosis by activating the NF-κB/MAPK signaling pathway (A) KEGG enrichment analysis was used to analyze the genes regulated by the downregulation of CSE1L in H1299 cell. (B and C) Apoptosis subset and TNF signaling were enriched in GSEA. (D and E) Gene expression of selected genes from the apoptosis subset and TNF signaling detected by qRT-PCR assay in CSE1L knockdown H1299 cell. (F) Schematic diagram of the NF-κB/MAPK signaling pathway. (G and H) Representative blots showing the protein levels of MAPK signaling pathway in the CSE1L knockdown H1299 or overexpressed A549 cells. β-actin was used as an internal control.

with cancer progression in various cancer types.^{26,29} Thus, CSE1L may have application value in the clinical diagnosis and treatment.

Nuclear-cytoplasmic transport is essential for tumor growth and development, affecting tumor suppressor protein and cell-cycle regulatory protein and inactivating cell apoptosis.³⁰ CSE1L expression has been

reported to correlate with cancer progression, and its abnormal distribution has been proposed to be a biomarker for cancer.³¹ CSE1L could interact with MSH6 and promote osteosarcoma progression via MSH6 in our previous study.¹⁹ However, the clinical significance and the biological functions of CSE1L in lung cancer remain elusive. In the present study, we have demonstrated that higher expression of CSE1L was

H1299 and PC-9 cells. (D and E) Confirmation of protein expression levels following si-P65 mix transfection by western blotting in CSE1L-overexpressed A549 and H292 cells. (F and G) Colony-formation assay was performed in the CSE1L-overexpressed A549 and H292 cells after si-P65 mix transfection. (H and I) Flow cytometry was employed to detect the apoptosis percentages in the CSE1L-overexpressed A549 and H292 cells after si-P65 mix transfection. Error bars represent the SD. *p < 0.05; **p < 0.01.

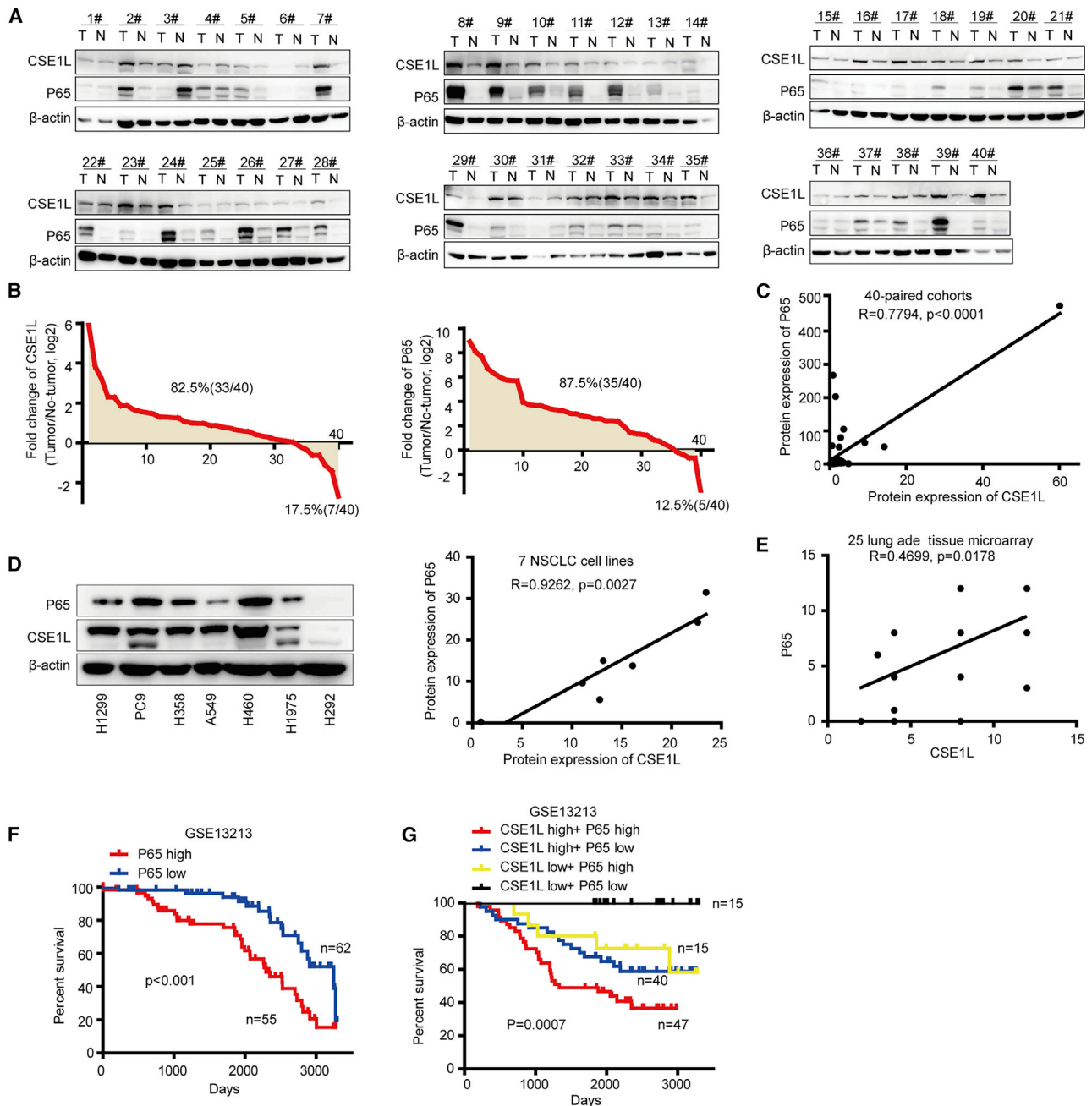


Figure 7. CSE1L expression paralleled that of P65 and correlated with the poor prognosis of NSCLC patients

(A) Photos of representative blots for CSE1L and P65 expression in 40 pairs of lung cancer and noncancerous tissues. (B) The fold changes of CSE1L and P65 protein expression levels in lung cancer tissues compared with noncancerous tissues. (C) The correlation between CSE1L and P65 expression in NSCLC tissues. (D) The protein levels of CSE1L and P65 and their correlation in NSCLC cells. (E) The correlation between CSE1L and P65 expression in 25 lung adenocarcinoma tissue microarrays. (F) The overall survival of P65 in GEO: GSE13213. (G) The overall survival of CSE1L and p65 in GEO: GSE13213.

observed in NSCLC tissues compared to that in adjacent noncancerous tissues. The increased CSE1L expression level was significantly associated with advanced tumor stages, as well as adverse patient outcome. It has been previously reported that CSE1L showed distinct localization patterns in different cell lines. CSE1L was consistently accumulated

in the nucleus of ovarian cancer cells, while it was mainly localized in the cytoplasm of the MCF7 breast cancer cells and was uniquely cytoplasmatic in the HT-29 colon carcinoma cells.^{32,33} CSE1L was also a secretory protein that existed in the body fluids of humans, especially in the blood of cancer patients.³⁴ However, the localization of CSE1L was

rarely studied in lung cancer. We observed that CSE1L was not only distributed in the nucleus of NSCLC cells but also in the cytoplasm. It was interesting that CSE1L was also observed in the membrane of NSCLC cells. In line with its different localization, CSE1L might play different roles in NSCLC. These findings indicated that CSE1L might serve as a clinical biomarker of prognosis in NSCLC and plays an important role in tumor progression.

CSE1L was first cloned in genes that rendered breast cancer cells resistant toward toxin.²¹ Some studies reported that CSE1L knockdown inhibited cell proliferation and increased cell apoptosis in colorectal cancer cells and gastric cancer cells.^{26,35} In our study, a series of *in vitro* and *in vivo* assays were conducted to clarify the biological functions of CSE1L in NSCLC cells. We found that CSE1L could increase the proliferation and protect lung cancer cells from apoptosis *in vitro* and *in vivo*. These findings matched with the knowledge that CSE1L was essential for cancer cell growth and apoptosis. CSE1L functioned in the mitotic spindle checkpoint, which was very important for the normal cell cycle.²⁸ Herein, it was interesting that downregulation of CSE1L had a different effect in NSCLC cells. CSE1L knockdown arrested the cell-cycle progression in the G2/M phase in H1299 cells and reduced the percentage of S phase in the PC-9 cells, and CSE1L overexpression had the opposite results both in G2/M phase and S phase. These results indicated that CSE1L promoted NSCLC cells' growth via affecting the cell cycle.

To date, the molecular mechanisms of how CSE1L promoted lung cancer cell proliferation and inhibited apoptosis have not been elucidated. Our data demonstrated that CSE1L could specifically interact with P65 to form a complex in the nuclei of NSCLC cells. The transcription factor NF- κ B regulated a variety of genes involved in immune and inflammatory responses, cell proliferation, tumorigenesis, cell survival, and tumor development.³⁶ The P65 also played a central role in the NF- κ B pathway.³⁷ The protein level of P65 was notably altered in the nucleus when CSE1L was knockdown or overexpressed, and its nuclear stabilization was protected from proteasomal degradation by CSE1L. We also showed that P65 attenuation significantly inhibited the proliferation and induced apoptosis of NSCLC cells *in vitro*, suggesting the indispensable role it has in lung cancer. P65 knockdown reduced the enhancement of CSE1L on NSCLC cells' proliferation and apoptosis evading. Survival analysis showed that high expression of P65 was significantly associated with a short survival time in lung cancer patients. Moreover, the shortest survival time was observed in the group with high expression of both CSE1L and P65. These findings further confirmed the correlation between CSE1L and P65 and indicated that the interaction was responsible for the oncogenic role of CSE1L.

So far, the affected signaling pathway with CSE1L on NSCLC cancer progression has been obscure and only a few signaling pathways have been reported. One study suggested that protein kinase B (AKT) activation forces the nuclear accumulation of CSE1L in the ovarian cancer cell, which was likely to induce oncogenic signals.³³ Another study revealed that CSE1L inhibition decreased melanocyte inducing transcription factor and suppressed glycoprotein nmb expression, thereby

activating the PI3K/Akt/mTOR and mitogen-activated protein kinase 7 (MEK)/mitogen-activated protein kinase 1 (ERK) signaling pathway and ultimately inhibiting the tumor growth and metastasis in gastric cancer.²⁶ In melanoma cells, CSE1L linked and controlled cyclic AMP (cAMP)/protein kinase A and Ras/ERK signal pathways and might be a potential target for melanomas treatment.³⁸ It has been well acknowledged that there are two distinct NF- κ B signaling pathways: (1) the classical pathway, primarily activated by pathogens and inflammatory mediators, and (2) the alternative pathway, which involves the NF- κ B-inducing kinase (NIK, also known as MAP3K14).³⁷ P65 played a key role in the regulation of MAPK signal pathway.^{39,40} It was reported that ERK was localized in the cytoplasm of resting cells, and extracellular stimulation inclined to induce a rapid and robust nuclear translocation of ERK.⁴¹ In our study, CSE1L activated ERK phosphorylation by effecting the protein expression of P65, then regulated the cell cycle and promoted NSCLC cell proliferation. JNK got involved in cancer cell apoptosis, proliferation, autophagy, and tumor immune evasion.⁴² Here, overexpression of CSE1L activated the JNK signal axis, thereby affecting the apoptotic signal. Consistently, we hypothesized that in the nucleus, CSE1L bound to the nuclear export signal (NES) on P65 and RAN in its active GTP-bound form (RAN-GTP). Meanwhile, CSE1L might promote the stabilization of P65. The complex was subsequently docked to NPC and passed through the NPC into the cytoplasm. Hydrolysis of RAN-GTP to RAN-GDP caused the disassembly of CSE1L-P65 complex and release of P65 and CSE1L into the cytoplasm, and then P65 activated the NF- κ B/MAPK pathway, resulting in the promotion of cell proliferation and the inhibition of cell apoptosis.

In summary, our findings demonstrate that CSE1L and P65 play important roles in the development of NSCLC. Meanwhile, CSE1L could interact with and affects the expression of P65 and then activates the NF- κ B/MAPK pathway, resulting in the promotion of NSCLC cell proliferation and the inhibition of cell apoptosis. More importantly, our study has suggested that CSE1L may serve as a promising therapeutic target for the prevention and treatment of NSCLC.

MATERIALS AND METHODS

Database analysis

We performed the ONCOMINE database combined with GEO database to screen NSCLC-associated NTRs. The expression data for 24 NTRs¹¹ were available from ONCOMINE. GEO datasets could be downloaded from the National Center for Biotechnology Information (NCBI). The survivals for the screened genes were analyzed in 117 lung adenocarcinoma patients (<https://www.ncbi.nlm.nih.gov/geo/query/acc.cgi?acc=GSE13213>) and 293 lung tumor samples (<https://www.ncbi.nlm.nih.gov/geo/query/acc.cgi?acc=GSE30219>). 503 lung adenocarcinoma patients from TCGA cohort (<https://cancergenome.nih.gov/>) was used to analyze the correlation between CSE1L mRNA levels and NSCLC clinicopathological features.

Human clinical specimens

Fresh human NSCLC tissues and matched adjacent noncancerous tissues for real-time PCR and western blot analyses were collected from

the Department of Cancer at Huashan Hospital affiliated with Fudan University, Shanghai, China between 2011 and 2018. During the operation, human surgical specimens were immediately frozen in liquid nitrogen and stored at -80°C for further investigation. All of the tissue specimens for this study were obtained with patient informed consent. The study was approved by the Ethics Committee of the Ethics Committee of Fudan University.

Tissue microarray

Two tissue microarrays containing 75 and 25 paired NSCLC tissues and matched adjacent noncancerous tissues was purchased from Shanghai Biochip (Shanghai, China). IHC staining was performed to detect the protein expression level of CSE1L in NSCLC tissues and matched noncancerous tissues. The average gray value of the image was used as a quantitative evaluation of the expression level using Image-Pro Plus 6.0 software. The proportion of the stained cells and the extent of the staining were used as the criteria for evaluation. The percentage of positive cells was scored as: $<5\%$ (0), $5\%–25\%$ (1), $25\%–50\%$ (2), $50\%–75\%$ (3), and $>75\%$ (4). The intensity of staining was scored as: no staining (0), light brown (1), brown (2), and dark brown (3). The final IHC scores were obtained using the traditional scoring method. IHC scores were calculated as the product of intensity (0 to 3) and the percentage of positive cells (0 to 4), yielding a range from 0 to 12.

Cell lines and cell culture

The human NSCLC cell lines H1299, PC-9, A549, H1975, H358, H460, and H292 and human embryonic kidney 293T cells were obtained from American Type Culture Collection (ATCC, Manassas, VA, USA). All cell lines were cultured according to ATCC protocols in Dulbecco's modified Eagle's medium (DMEM) or Roswell Park Memorial Institute (RPMI) 1640 supplemented with 10% fetal bovine serum (FBS; Biowest, South America origin), 100 $\mu\text{g}/\text{mL}$ penicillin (Sigma-Aldrich, USA), and 100 $\mu\text{g}/\text{mL}$ streptomycin (Sigma-Aldrich, USA) at 37°C in a humidified incubator under 5% carbon dioxide. These cell lines were mycoplasma-free and authenticated by quality examinations of morphology and growth profile.

RNA extraction and real-time PCR assay

Total RNA was extracted from the lung cancer cells and tissues using TRIzol Reagent (Invitrogen, Carlsbad, CA, USA) according to the manufacturer's protocol. cDNA was synthesized by random primers and the PrimeScript RT Reagent Kit (Takara, Dalian, China). The primer sequences for real-time PCR are shown in Table S4. Real-time PCR was performed using SYBR Premix Ex Tag (Takara, Dalian, China). The PCR conditions were as follows: 95°C for 15 s followed by 40 cycles of 95°C for 5 s and 60°C for 30 s. β -actin was used as the internal control.

Vector construction and RNA interference

siRNA oligonucleotides for CSE1L and P65 were designed and synthesized by RiboBio (Guangzhou, China). The sequences for the siRNAs are shown in Table S5. Transient transfection was performed using Lipofectamine 2000 Reagent (Invitrogen, Carlsbad, USA) ac-

ording to the manufacturer's instructions. After transfection for 48 h, the cells were used for functional assays, including apoptosis, migration, invasion, colony formation, RNA extraction, and western blot.

Because si-CSE1L 2# showed more effective interference efficiency, so we selected the sequence to construct a stable interference CSE1L cell lines. The coding sequences (CDS) of human CSE1L were commercially synthesized (GENEWIZ) and then were cloned and inserted into the lentiviral expression vector pWPXL. To produce lentivirus containing CSE1L, we cotransfected 293T cells with the pWPXL-CSE1L and the lentiviral vector packaging system using Lipofectamine 2000.

Protein extraction and western blotting

Cell and tissue proteins were extracted using T-PER Protein Extraction Reagent (Thermo Scientific, USA) with a phosphatase inhibitor cocktail (Roche Applied Science, Switzerland) and a proteinase inhibitor cocktail (Roche Applied Science, Switzerland). We used the MinuteTM Cytoplasmic and Nuclear Extraction Kit (Invent Biotechnologies, USA) to separate the nuclear and cytoplasmic. The protein concentrations were determined using the Pierce BCA Protein Assay Kit (Thermo Scientific, USA). Proteins were separated by SDS-PAGE gels and transferred to nitrocellulose (NC) filter membranes (Millipore, MA, USA) or polyvinylidene fluoride (PVDF) membranes (Millipore, MA, USA). The membranes were incubated with primary antibodies overnight at 4°C and probed with secondary antibodies at room temperature for 1~2 h. The antibodies used were shown in Table S6.

Cell proliferation and colony-formation assay

The relative cell proliferation was monitored using CCK-8 (Dojindo, Japan) according to the manufacturer's protocol. Briefly, cells were seeded in 96-well plates at 1×10^3 cells per well. According to the manufacturer's instructions, 10 μL of CCK-8 solution and 100 μL medium was added to each well, and the mixture was incubated at 37°C for 2 h. The absorbance was measured at 450 nm.

For the colony-formation assay, a total of 0.5×10^3 cells was seeded in 6-well plates and cultured at 37°C in a humidified incubator at 5% carbon dioxide. 2 weeks later, the cell colonies were washed with phosphate-buffered saline (PBS), fixed with methanol, and stained with 0.1% crystal violet (1 mg/mL) for 30 min. All of the experiments were repeated in triplicate and assessed under a light microscope.

Flow cytometry for cell apoptosis and cell-cycle analysis

The human NSCLC cell lines stably interference or overexpressed of CSE1L, and cells transfected with P65 si-RNAs were used for the experiments. A flow cytometer (BD LSR II, BD Biosciences, USA) was used to detect the cell phenotype. Apoptosis was measured via the Apoptosis Detection Kit (BD Biosciences, USA) according to the manufacturer's protocol. The data was analyzed using FlowJo software version 8.6.3 (FlowJo, USA). Cell-cycle distribution was

measured by the PI Cell Cycle Detection Kit (Beyotime Biotechnology, China) according to the manufacturer's protocol. The results were analyzed using ModFit software (BD Biosciences, USA).

Cell migration and invasion assays

Cell migration and invasion assays were performed by Transwell filter chambers (BD Biosciences, NJ, USA). For migration assays, 5×10^4 cells in 200 μ L of serum-free culture medium were suspended into the upper chamber with the noncoated membrane. For invasion assays, 1×10^5 cells in 200 μ L of serum-free culture medium were placed into the upper chamber with the Matrigel-coated membrane diluted with serum-free culture medium. An 800 μ L culture medium supplemented with 10% FBS was added in the lower chamber. After incubation at 37°C in a humidified incubator under 5% carbon dioxide, the cells in the bottom surface of the membrane were fixed with 100% methanol, stained with 0.1% crystal violet for 30 min, and counted under a light microscope (Olympus, Japan).

Immunofluorescence

Cells were plated in 6-well plates on glass coverslips. The cells were fixed with 4% formaldehyde for 15 min at 4°C and then infiltrated with 0.3% Triton X-100 for 15 min. After washing three times with PBS, the wells were treated with blocking solution for 30 min and then incubated overnight with anti-CSE1L (Abcam, 1:50) and anti-P65 (Cell Signaling Technology (CST), 1:50) antibody at 4°C. After incubation with the secondary antibody (anti-rabbit [Invitrogen, 1:300], anti-mouse [Invitrogen, 1:150]) at room temperature for 1 h, 4', 6-diamidino-2-phenylindole (DAPI) was used to stain the nucleus. A confocal laser scanning microscope (Leica TCS-SP5, Leica Microsystems, Germany) was used to observe the images.

colP and MS

When the confluence of cells in the culture plate reached more than 90%, the cells were scraped off directly with a cell scraper using ice-cold radioimmunoprecipitation assay (RIPA) lysis buffer (Beyotime Institute of Biotechnology, Shanghai, China) with protease and protein phosphatase inhibitors (Roche Applied Science, Switzerland). 3 mg of protein were pre-cleared with 30 μ L of protein A/G magnetic beads (Millipore, MA, USA) at 4°C for 2 h. The beads were removed, and 5 μ L of the primary antibody (CSE1L or P65) or isotype immunoglobulin G (IgG) was added to the supernatant at 4°C overnight with gentle mixing on a rocking platform to capture the fusion proteins. Then, 40 μ L of protein A/G magnetic beads was added to each immunoprecipitation mixture for 4 h at 4°C. The magnetic beads were collected by placing the tube in the appropriate magnetic separator. The beads were washed three times with PBS/0.1% Triton. The magnetic beads isolated using a magnetic rack and then boiled in 2 \times sodium dodecyl sulfate (SDS) loading buffer. The bound fusion proteins were separated by SDS-PAGE and stained with a Silver Staining Kit (Beyotime Biotechnology, Shanghai, China). The proteins in the SDS-PAGE were digested with trypsin and then analyzed by Triple TOF 5,600 mass spectrometer (AB Sciex, TX, USA). Protein identification was performed using Protein Pilot 4.5 (AB Sciex, TX, USA).

In vivo tumor growth

All animal experiments were approved by the Animal Ethics Committee of the Shanghai Cancer Institute. 6- to 8-week-old female BALB/c-nu/nu mice were bred by Shanghai Cancer Institute (Shanghai, China) and housed in specific pathogen-free (SPF) conditions in a laboratory animal facility.

For the *in vivo* xenograft assays, 3×10^6 A549 cells and H292 cells stably expressing CSE1L or the lentiviral vector and 2×10^6 PC-9 cells and H1299 cells stably expressing shCSE1L or the negative control were separately subcutaneously inoculated into the dorsal right flanks of the nude mice (6 or 8 per group). The tumor size was measured two times every week. The tumor volume (V) was measured by calipers and calculated according to the following formula: (length \times width \times width)/2. After 8 or 10 weeks, the mice were sacrificed, and the tumors were weighed.

Statistical analysis

All experiments were performed independently at least three times or as indicated in the figures. Data are presented as the mean \pm standard deviation (SD) or the mean \pm standard error of the mean (SEM). Mean values between groups were assessed by two-tailed Student's t tests. Survival times were analyzed using the log-rank test. The correlation of CSE1L and P65 expression was examined by Spearman's correlation test. Differences were considered statistically significant at $p < 0.05$.

SUPPLEMENTAL INFORMATION

Supplemental information can be found online at <https://doi.org/10.1016/j.omto.2021.02.015>.

ACKNOWLEDGMENTS

We thank all individuals who take part in this research. This work was supported by The National Natural Science Foundation of China (grant numbers 81802894 to H.L., 81772481 to M.Y., and 81802270 to T.Y.).

AUTHOR CONTRIBUTIONS

H. Lin, M.Y., and H. Li were in responsible for the design of the study and wrote the manuscript; H.L. and J.L. cultured cellular experiments, performed western blot validation, and analyzed the data; T.Y. performed RT-PCR and the study of the signaling pathway; D.C. participated in the mass spectrometry analysis and bioinformatic analysis; X.Z. helped conduct the migration and invasion assay; F.Z. and Q.G. were in charge of the animal imaging detection. M.Z. and H.K. helped some animal experiments; all of the authors reviewed the manuscript before submission and approved the final manuscript.

DECLARATION OF INTERESTS

The authors declare no competing interests.

REFERENCES

1. Bray, F., Ferlay, J., Soerjomataram, I., Siegel, R.L., Torre, L.A., and Jemal, A. (2018). Global cancer statistics 2018: GLOBOCAN estimates of incidence and mortality worldwide for 36 cancers in 185 countries. *CA Cancer J. Clin.* 68, 394–424.

2. Travis, W.D. (2020). Lung Cancer Pathology: Current Concepts. *Clin. Chest Med.* 41, 67–85.
3. Travis, W.D., Brambilla, E., Nicholson, A.G., Yatabe, Y., Austin, J.H.M., Beasley, M.B., Chirieac, L.R., Dacic, S., Duhig, E., Flieder, D.B., et al.; WHO Panel (2015). The 2015 World Health Organization Classification of Lung Tumors: Impact of Genetic, Clinical and Radiologic Advances Since the 2004 Classification. *J. Thorac. Oncol.* 10, 1243–1260.
4. Lynch, T.J., Bell, D.W., Sordella, R., Gurubhagavatula, S., Okimoto, R.A., Brannigan, B.W., Harris, P.L., Haserlat, S.M., Supko, J.G., Haluska, F.G., et al. (2004). Activating mutations in the epidermal growth factor receptor underlying responsiveness of non-small-cell lung cancer to gefitinib. *N. Engl. J. Med.* 350, 2129–2139.
5. Kwak, E.L., Bang, Y.J., Camidge, D.R., Shaw, A.T., Solomon, B., Maki, R.G., Ou, S.H., Dezube, B.J., Jänne, P.A., Costa, D.B., et al. (2010). Anaplastic lymphoma kinase inhibition in non-small-cell lung cancer. *N. Engl. J. Med.* 363, 1693–1703.
6. Zhang, K., Ma, Y., Guo, Y., Sun, T., Wu, J., Pangeni, R.P., Lin, M., Li, W., Horne, D., and Raz, D.J. (2020). Cetuximab-Triptolide Conjugate Suppresses the Growth of EGFR-Overexpressing Lung Cancers through Targeting RNA Polymerase II. *Mol. Ther. Oncolytics* 18, 304–316.
7. Hirsch, F.R., Scagliotti, G.V., Mulshine, J.L., Kwon, R., Curran, W.J., Jr., Wu, Y.L., and Paz-Ares, L. (2017). Lung cancer: current therapies and new targeted treatments. *Lancet* 389, 299–311.
8. Beck, M., and Hurt, E. (2017). The nuclear pore complex: understanding its function through structural insight. *Nat. Rev. Mol. Cell Biol.* 18, 73–89.
9. Cole, C.N., and Scarcelli, J.J. (2006). Transport of messenger RNA from the nucleus to the cytoplasm. *Curr. Opin. Cell Biol.* 18, 299–306.
10. Fried, H., and Kutay, U. (2003). Nucleocytoplasmic transport: taking an inventory. *Cell. Mol. Life Sci.* 60, 1659–1688.
11. Baade, I., and Kehlenbach, R.H. (2019). The cargo spectrum of nuclear transport receptors. *Curr. Opin. Cell Biol.* 58, 1–7.
12. Mahipal, A., and Malafa, M. (2016). Importins and exportins as therapeutic targets in cancer. *Pharmacol. Ther.* 164, 135–143.
13. Gravina, G.L., Senapedis, W., McCauley, D., Baloglu, E., Shacham, S., and Festuccia, C. (2014). Nucleo-cytoplasmic transport as a therapeutic target of cancer. *J. Hematol. Oncol.* 7, 85.
14. Kosyna, F.K., and Depping, R. (2018). Controlling the Gatekeeper: Therapeutic Targeting of Nuclear Transport. *Cells* 7, 221.
15. Azmi, A.S., Uddin, M.H., and Mohammad, R.M. (2020). The nuclear export protein XPO1 - from biology to targeted therapy. *Nat. Rev. Clin. Oncol.* 18, 152–169.
16. Azizian, N.G., and Li, Y. (2020). XPO1-dependent nuclear export as a target for cancer therapy. *J. Hematol. Oncol.* 13, 61.
17. Ding, C., Li, C., Wang, H., Li, B., and Guo, Z. (2013). A miR-SNP of the XPO5 gene is associated with advanced non-small-cell lung cancer. *Oncotargets Ther.* 6, 877–881.
18. Geng, J.Q., Wang, X.C., Li, L.F., Zhao, J., Wu, S., Yu, G.P., and Zhu, K.J. (2016). MicroRNA-related single-nucleotide polymorphism of XPO5 is strongly correlated with the prognosis and chemotherapy response in advanced non-small-cell lung cancer patients. *Tumour Biol.* 37, 2257–2265.
19. Cheng, D.D., Lin, H.C., Li, S.J., Yao, M., Yang, Q.C., and Fan, C.Y. (2017). CSE1L interaction with MSH6 promotes osteosarcoma progression and predicts poor patient survival. *Sci. Rep.* 7, 46238.
20. Scherf, U., Pastan, I., Willingham, M.C., and Brinkmann, U. (1996). The human CAS protein which is homologous to the CSE1 yeast chromosome segregation gene product is associated with microtubules and mitotic spindle. *Proc. Natl. Acad. Sci. USA* 93, 2670–2674.
21. Brinkmann, U., Brinkmann, E., Gallo, M., and Pastan, I. (1995). Cloning and characterization of a cellular apoptosis susceptibility gene, the human homologue to the yeast chromosome segregation gene CSE1. *Proc. Natl. Acad. Sci. USA* 92, 10427–10431.
22. Behrens, P., Brinkmann, U., and Wellmann, A. (2003). CSE1L/CAS: its role in proliferation and apoptosis. *Apoptosis* 8, 39–44.
23. Liao, C.F., Lin, S.H., Chen, H.C., Tai, C.J., Chang, C.C., Li, L.T., Yeh, C.M., Yeh, K.T., Chen, Y.C., Hsu, T.H., et al. (2012). CSE1L, a novel microvesicle membrane protein, mediates Ras-triggered microvesicle generation and metastasis of tumor cells. *Mol. Med.* 18, 1269–1280.
24. Dong, Q., Li, X., Wang, C.Z., Xu, S., Yuan, G., Shao, W., Liu, B., Zheng, Y., Wang, H., Lei, X., et al. (2018). Roles of the CSE1L-mediated nuclear import pathway in epigenetic silencing. *Proc. Natl. Acad. Sci. USA* 115, E4013–E4022.
25. Wang, Y.S., Peng, C., Guo, Y., and Li, Y. (2020). CSE1L promotes proliferation and migration in oral cancer through positively regulating MITF. *Eur. Rev. Med. Pharmacol. Sci.* 24, 5429–5435.
26. Li, Y., Yuan, S., Liu, J., Wang, Y., Zhang, Y., Chen, X., and Si, W. (2020). CSE1L silence inhibits the growth and metastasis in gastric cancer by repressing GPNMB via positively regulating transcription factor MITF. *J. Cell. Physiol.* 235, 2071–2079.
27. Tanaka, T., Ohkubo, S., Tatsuno, I., and Prives, C. (2007). hCAS/CSE1L associates with chromatin and regulates expression of select p53 target genes. *Cell* 130, 638–650.
28. Liu, C., Wei, J., Xu, K., Sun, X., Zhang, H., and Xiong, C. (2019). CSE1L participates in regulating cell mitosis in human seminoma. *Cell Prolif.* 52, e12549.
29. Tai, C.J., Hsu, C.H., Shen, S.C., Lee, W.R., and Jiang, M.C. (2010). Cellular apoptosis susceptibility (CSE1L/CAS) protein in cancer metastasis and chemotherapeutic drug-induced apoptosis. *J. Exp. Clin. Cancer Res.* 29, 110.
30. Tran, E.J., King, M.C., and Corbett, A.H. (2014). Macromolecular transport between the nucleus and the cytoplasm: Advances in mechanism and emerging links to disease. *Biochim. Biophys. Acta* 1843, 2784–2795.
31. Jiang, M.C. (2016). CAS (CSE1L) signaling pathway in tumor progression and its potential as a biomarker and target for targeted therapy. *Tumour Biol.* 37, 13077–13090.
32. Lorenzato, A., Martino, C., Dani, N., Oligschläger, Y., Ferrero, A.M., Biglia, N., Calogero, R., Olivero, M., and Di Renzo, M.F. (2012). The cellular apoptosis susceptibility CAS/CSE1L gene protects ovarian cancer cells from death by suppressing RASSF1C. *FASEB J.* 26, 2446–2456.
33. Lorenzato, A., Biolatti, M., Delogu, G., Capobianco, G., Farace, C., Dessole, S., Cossu, A., Tanda, F., Madeddu, R., Olivero, M., and Di Renzo, M.F. (2013). AKT activation drives the nuclear localization of CSE1L and a pro-oncogenic transcriptional activation in ovarian cancer cells. *Exp. Cell Res.* 319, 2627–2636.
34. Tsao, T.Y., Tsai, C.S., Tung, J.N., Chen, S.L., Yue, C.H., Liao, C.F., Wang, C.C., and Jiang, M.C. (2009). Function of CSE1L/CAS in the secretion of HT-29 human colorectal cells and its expression in human colon. *Mol. Cell. Biochem.* 327, 163–170.
35. Zhu, J.H., Hong, D.F., Song, Y.M., Sun, L.F., Wang, Z.F., and Wang, J.W. (2013). Suppression of cellular apoptosis susceptibility (CSE1L) inhibits proliferation and induces apoptosis in colorectal cancer cells. *Asian Pac. J. Cancer Prev.* 14, 1017–1021.
36. Oeckinghaus, A., and Ghosh, S. (2009). The NF-kappaB family of transcription factors and its regulation. *Cold Spring Harb. Perspect. Biol.* 1, a000034.
37. Jimi, E., Fei, H., and Nakatomi, C. (2019). NF-κB Signaling Regulates Physiological and Pathological Chondrogenesis. *Int. J. Mol. Sci.* 20, 6275.
38. Lee, W.R., Shen, S.C., Wu, P.R., Chou, C.L., Shih, Y.H., Yeh, C.M., Yeh, K.T., and Jiang, M.C. (2016). CSE1L Links cAMP/PKA and Ras/ERK pathways and regulates the expressions and phosphorylations of ERK1/2, CREB, and MITF in melanoma cells. *Mol. Carcinog.* 55, 1542–1552.
39. Du, X., Wang, S., Liu, X., He, T., Lin, X., Wu, S., Wang, D., Li, J., Huang, W., and Yang, H. (2020). MiR-1307-5p targeting TRAF3 upregulates the MAPK/NF-κB pathway and promotes lung adenocarcinoma proliferation. *Cancer Cell Int.* 20, 502.
40. Tang, F., Wang, H., Chen, E., Bian, E., Xu, Y., Ji, X., Yang, Z., Hua, X., Zhang, Y., and Zhao, B. (2019). LncRNA-ATB promotes TGF-β-induced glioma cells invasion through NF-κB and P38/MAPK pathway. *J. Cell. Physiol.* 234, 23302–23314.
41. Maik-Rachline, G., Hacohen-Lev-Ran, A., and Seger, R. (2019). Nuclear ERK: Mechanism of Translocation, Substrates, and Role in Cancer. *Int. J. Mol. Sci.* 20, 1194.
42. Wu, Q., Wu, W., Fu, B., Shi, L., Wang, X., and Kuca, K. (2019). JNK signaling in cancer cell survival. *Med. Res. Rev.* 39, 2082–2104.